Available online at www.sciencedirect.com
ScienceDirect
Journal of Catalysis 245 (2007) 75–83
JOURNAL OF CATALYSIS
www.elsevier.com/locate/jcat

Studies on the identification of the heteropoly acid generated in the H_3PO_4–WO_3–Nb_2O_5 catalyst and its thermal transformation process

Kazu Okumura *, Katsuhiko Yamashita, Kazuhiro Yamada, Miki Niwa

Department of Materials Science, Faculty of Engineering, Tottori University, Koyama-cho, Tottori 680-8552, Japan

Received 16 June 2006; revised 22 September 2006; accepted 25 September 2006

Available online 25 October 2006

Abstract

The precursor of the mixed metal oxide catalyst composed of H_3PO_4–WO_3–Nb_2O_5, which exhibits excellent activity in Friedel–Crafts alkylations, was identified with ^{31}P NMR. It was revealed that the Keggin-type mixed heteropoly acid, $H_4PNbW_{11}O_{40}$, was spontaneously generated during preparation of the H_3PO_4–WO_3–Nb_2O_5 catalyst. The partial decomposition of $H_4PNbW_{11}O_{40}$ occurred in the temperature range of 673–823 K to give an amorphous oxide that had a Brønsted acid character. Based on the results of structural and acidic studies, the active species obtained through the calcination of H_3PO_4–WO_3–Nb_2O_5 was ascribed to the transient state in the course of the thermal decomposition of the $H_4PNbW_{11}O_{40}$ over the WO_3–Nb_2O_5 support. In fact, the catalyst prepared by mixing $H_4PNbW_{11}O_{40}$, niobic oxalate, and ammonium tungstate solutions, followed by calcination at 773 K, exhibited excellent activity in the Friedel–Crafts acylation of anisole with carboxylic acids.

Keywords: Heteropoly acid; Keggin unit; NMR; XRD; NH_3-TPD; XAFS

1. Introduction

Heteropoly acids (HPAs) are promising materials having strong acidity as well as oxidizing ability; thus, they are used as catalysts for various kinds of organic synthesis, including selective oxidation and acid-catalyzed organic reactions [1–4]. It has been recognized that a major drawback of HPA is its low thermal stability when applied to high-temperature reactions. Although the thermal stability depends on the structure and composition of HPAs, the total decomposition of Keggin structure generally occurs at temperatures up to 723–823 K to give the mixed oxides composed of HPAs [5]. In the case of $H_3PW_{12}O_{40}$ (designated as HPW), the deactivation begins at a lower temperature in many catalytic reactions despite the stability of the Keggin structure up to 823 K [6]. However, several groups have found that the thermally treated HPAs exhibits unique catalytic activities. Of particular interest is the structural transformation of the Mo,V-mixed HPA (i.e., $H_4PVMo_{11}O_{40}$) with a Keggin structure, because of the high activity in the oxidative dehydrogenation of isobutyric acid to methacrylic acid or the oxidation of methacrolein to methacrylic acid [5,7,8]. Infrared (IR) studies of $H_4PVMo_{11}O_{40}$ have revealed that the transformation takes place via the release of vanadium from the host Keggin structure to give $PMo_{12}H$ and vanadophosphate species [9]. Halligudi et al. reported that the HPW/ZrO_2 or HPW/ZrO_2/MCM-41 calcined at 1023 K exhibited high activity in various solid acid reactions [10,11]. Two-step thermal decomposition of the Keggin ion was proposed over the magnesium salt of a HPA ($HMgPMo_{12}O_{40}$) that was induced by stabilizing effect of intermediate planar oxide species [12]. We have recently found that the partially decomposed heteropoly acid derived from ternary mixed oxides (H_3PO_4–WO_3–Nb_2O_5; Cat A hereinafter) exhibited excellent catalytic performance, showing facile reusability as well as high activity in the benzylation of anisole using benzyl alcohol [13,14]. The activity of Cat A was four times higher than that of the montmorillonite-K10 clay treated with sulfuric acid, which has been recognized as an active catalyst for these kinds of reactions. The dependence of the catalytic activity of Cat A on the calcination temperature was remarkably sharp, with the optimum condition at-

* Corresponding author. Fax: +81 857 31 5684.
E-mail address: okmr@chem.tottori-u.ac.jp (K. Okumura).

0021-9517/$ – see front matter
doi:10.1016/j.jcat.2006.09.021

tained at 773 K. Detailed studies of structure and acid properties revealed that the active species was derived from a heteropoly acid.

In this study, to assign the precursor for the Cat A, first ^{31}P NMR spectrum of the HPAs extracted from Cat A was measured. Then the thermal decomposition process of the $H_4PNbW_{11}O_{40}$ (designated as HPNbW), which appeared to be the primary precursor of Cat A, was followed in terms of structural and acidic characterizations by changing the calcination temperature stepwise. The experiments were carried out in comparison with HPW that lacked Nb atoms in the structure. We believe that the role of the Nb atom present in the Keggin structure can be elucidated through the comparison with HPW. Moreover, a catalyst was prepared by mixing HPNbW, niobium oxalate, and ammonium tungstate (HPNbW–WO_3–Nb_2O_5, or Cat B), followed by calcination in air. The catalyst was applied to the Friedel–Crafts acylation of anisole with carboxylic acids to extend the possibility of Cat A, in which the active species was derived from HPNbW.

2. Experimental

2.1. Preparation of the H_3PO_4–WO_3–Nb_2O_5 (Cat A)

Cat A was prepared as described previously [13]. Niobium oxalate was prepared by dissolving 1.27 g of niobic acid (supplied by CBMM Co.) in an oxalic acid (Wako Chemical Ltd., 4.77 g) solution (100 ml) on a hot plate at 353 K. $(NH_4)_{10}W_{12}O_{41}\cdot 5H_2O$ (Wako Chemical Ltd., 1.69 g) was dissolved in deionized water (100 ml). The solutions of niobium oxalate and $(NH_4)_{10}W_{12}O_{41}$ were mixed together, followed by the addition of 85% phosphoric acid (0.22 g). The admixture solution was evaporated on a hot plate with continuous stirring. The obtained solid was calcined with an electric furnace for 3 h in air. The composition of the Cat A calcined at 773 K was determined to be 8.6 wt% H_3PO_4, 54.8 wt% WO_3, and 36.6 wt% Nb_2O_5 as determined by ICP analysis. The surface area of Cat A calcined at 773 K was determined to be 58 $m^2\ g^{-1}$ by BET method.

2.2. Synthesis of $HPNbW\cdot 13H_2O$

Synthesis of HPNbW was carried out in a similar manner as for HPW except the addition of niobic oxalate as a source of Nb [15]. A mixed aqueous solution (total volume, 160 ml) of $Na_2WO_4\cdot 2H_2O$ (100 g), $Na_2HPO_4\cdot 12H_2O$ (50 g), and niobic oxalate was stirred 353 K for 4 h, followed by the addition of a 24% HCl solution (150 ml). The chemicals other than niobic oxalate were supplied by Wako Chemical Ltd. The niobium oxalate solution was prepared according to the same manner as for the preparation of Cat A; that is, 1.27 g of niobic acid (supplied by CBMM Co.) was dissolved in an oxalic acid (Wako Chemical Ltd., 4.77 g) solution (100 ml) on a hot plate. The mixed solution of three components was then evaporated to give 100 ml in volume. After cooling down to the room temperature, the concentrated solution was transferred to a separator funnel. The product solution was extracted as a precipitate in the bottom of the funnel by the addition of diethylether and a small amount of conc. HCl. According to the ICP and TG analysis, the composition of the obtained heteropoly acid was determined to be P:Nb:W:H_2O = 1.1:1.0:11.0:13.2, which almost agreed with the formula of $H_4PNbW_{11}O_{40}\cdot 13H_2O$. The number of the constitutional water was close to that of $H_3PW_{12}O_{40}\cdot 13H_2O$ having triclinic phase.

2.3. Preparation and catalytic reactions of the HPNbW–WO_3–Nb_2O_5 (Cat B)

The preparation of Cat B was carried out in a similar manner as for Cat A, but using HPNbW as the precursor for the active species. The solutions of HPNbW, ammonium tungstate, and niobic oxalate were mixed together, followed by evaporation of water on a hot plate. The solution of HPNbW was prepared by dissolution of 5.43 g of $HPNbW\cdot 13H_2O$ in a 100 ml of ion-exchanged water. HPNbW was synthesized as described in Section 2.2. The solution of ammonium tungstate was prepared by dissolving 5.07 g of $(NH_4)_{10}W_{12}O_{41}\cdot 5H_2O$ (Wako Chemicals Ltd.) in a 100 ml of ion-exchanged water. The niobium oxalate solution was prepared by dissolving niobic acid (3.81 g, CBMM Co.) in the oxalic acid (14.3 g, Wako Chemical Ltd.) solution (100 ml), as described in Section 2.1. The solid thus obtained was finally calcined at 773 K for 3 h. The catalyst composition of the catalyst was 40 wt% HPNbW, 36 wt% WO_3, and 24 wt% Nb_2O_5. Catalyst amounts of 0.5 g were used for the acylation of anisole with benzoic acid (Scheme (1)) or butanoic acid (Scheme (2)):

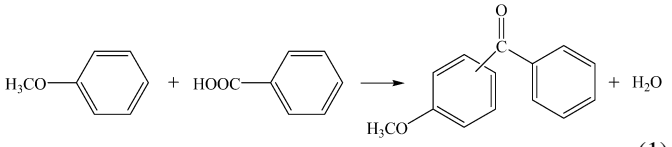

(1)

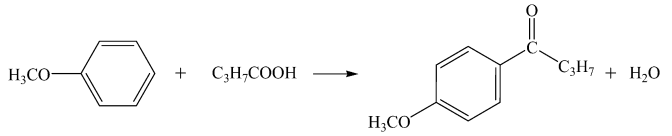

(2)

The reaction was performed over catalysts (0.5 g) using 10 g of anisole and 2.0 mmol of benzoic acid (reaction temperature, 413 K) or butanoic acid (reaction temperature, 428 K) in an oil bath for 3 h in N_2 atmosphere. All reagents were supplied by Wako Chemical Ltd. Anisole was dried over 3A molecular sieves. Catalyst pretreatments were not done before the reactions. For recycling, the catalyst separated by filtration was used for the repeat reactions. The reactions were also performed over H-β zeolite (PQ, $Si/Al_2 = 20$), which was dehydrated in an N_2 flow at 573 K. The products were analyzed by gas chromatography using a Shimadzu GC-2010 equipped with a MDN-12 capillary column and a flame ionization detector. In the analysis, tridecane was used as an internal standard.

2.4. ^{31}P NMR measurement

^{31}P NMR measurement was carried out using a JEOL JNM-ECP500 device. For sample preparation, HPAs were extracted from Cat A (0.1 g; calcination temperature, 673 K) using D_2O (3.4 g) as a solvent. The solution was concentrated to 1/3 volume on a hot plate before the NMR measurement. The W extracted into the D_2O from the original Cat A was calculated to be 53% as measured by ICP. The chemical shifts were referenced with respect to external 85% H_3PO_4.

2.5. XRD measurement

The crystalline structure was analyzed by XRD in ambient conditions using a Rigaku Mini-Flex Plus X-ray diffractometer with Cu$K\alpha$ radiation.

2.6. IR measurement

FTIR measurement was carried out using a Perkin–Elmer Spectrum One spectrometer. Before measurement, the sample was pressed to form pellets after dilution with KBr by a weight factor of 10. IR spectra were recorded in a transmission mode with the resolution of 4 cm^{-1}.

2.7. W-L_1, -L_3 XAFS measurement and analysis

The W-L_1 (12.1 keV) and W-L_3 edge (10.2 keV) XAFS data were collected at BL01B1 station in a SPring-8 with the approval of the Japan Synchrotron Radiation Research Institute (JASRI) (proposal 2005B0022-NXa-np). The storage ring was operated at 8 GeV. A Si(111) single crystal was used to obtain a monochromatic X-ray beam. The measurement was carried out in the quick mode. Two ion-chambers filled with N_2 and N_2(50%)/Ar(50%) were used for I_0 and I, respectively. The wafer-form samples were pretreated at 673 K under an N_2 flow. After the sample was cooled to room temperature, it was sealed in a polyethylene bag in a glove box. The data analysis was performed using the REX2000 version 2.0.4 program (Rigaku). Fourier transformation of $k^3\chi(k)$ data were performed in the k range of 20–150 nm^{-1} for analysis of the W-L_3 edge spectra.

2.8. Temperature-programmed desorption of ammonia

Temperature-programmed desorption (TPD) of ammonia was measured over thermally treated HPAs using a BEL Japan TPD-AT-1 device. The samples were evacuated at 373–673 K (below the calcination temperatures) before measurement. 13.3 kPa of ammonia was equilibrated with the pretreated sample at 373 K. The TPD data were collected at temperature ramp rate of 10 K min^{-1}. A mass spectrometer was used to measure the desorbed NH_3 at $m/e = 16$.

2.9. IR spectra of adsorbed pyridine

IR spectra of adsorbed pyridine were measured using a quartz cell connected to a vacuum line. The sample placed in a quartz holder was evacuated at 473 K, followed by admission of 2.0 kPa of pyridine to the vacuum line. After evacuation of the pyridine, IR spectra were measured at room temperature using a Perkin–Elmer Spectrum One spectrometer with a resolution of 4 cm^{-1}.

3. Results

3.1. ^{31}P NMR of the extracts of H_3PO_4–WO_3–Nb_2O_5 (Cat A) and the synthesized HPNbW

Fig. 1a shows the ^{31}P NMR spectrum of the Cat A extracts. The extraction was carried out over Cat A calcined at 673 K using D_2O as a solvent at room temperature. At this calcination temperature, HPAs remained intact, as reported previously [13]. The single peak appearing at −15.3 ppm can be assigned to the HPW, as indicated after comparison with the authentic compound. Moreover, a single peak and triple peaks appeared at −13.8 ppm and around −12.3 ppm, respectively. The relative concentration of HPAs at −15.3, −13.8, and −12.3 ppm was determined to be 28:54:18 based on the area of the peaks, showing that the substance corresponding to the −13.8 ppm dominated in solution.

The ^{31}P NMR spectrum of the HPNbW dissolved in D_2O is shown in Fig. 1b. A single peak appeared at −13.8 ppm, in agreement with that found in the extracts. Although it was difficult to rule out the possibility of initial formation of the lacunary PW_{11} species, followed by its insertion with Nb(V) to yield the HPNbW, the coincidence in the peak position suggested that the major component present in Cat A calcined at lower temperature could be ascribed to the HPNbW.

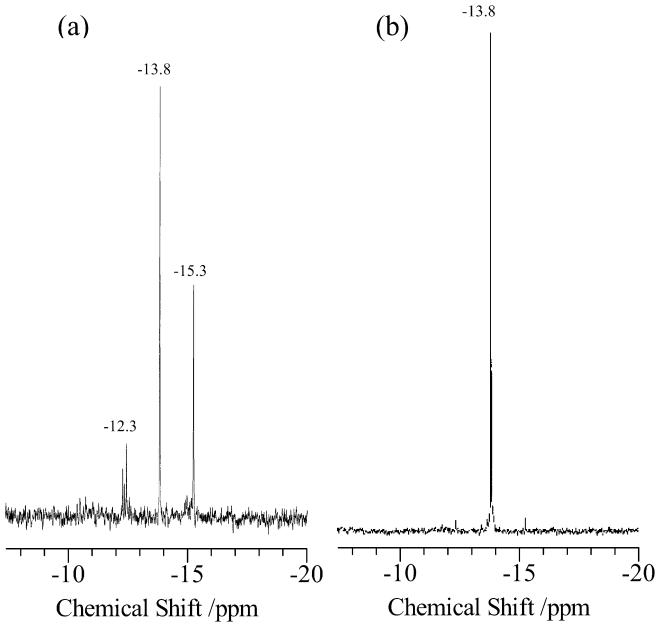

Fig. 1. ^{31}P NMR of (a) HPAs extracted from H_3PO_4–WO_3–Nb_2O_5 (Cat A) calcined at 673 K and (b) synthesized HPNbW. D_2O was used as a solvent. The chemical shift was referenced with the respect to the external H_3PO_4.

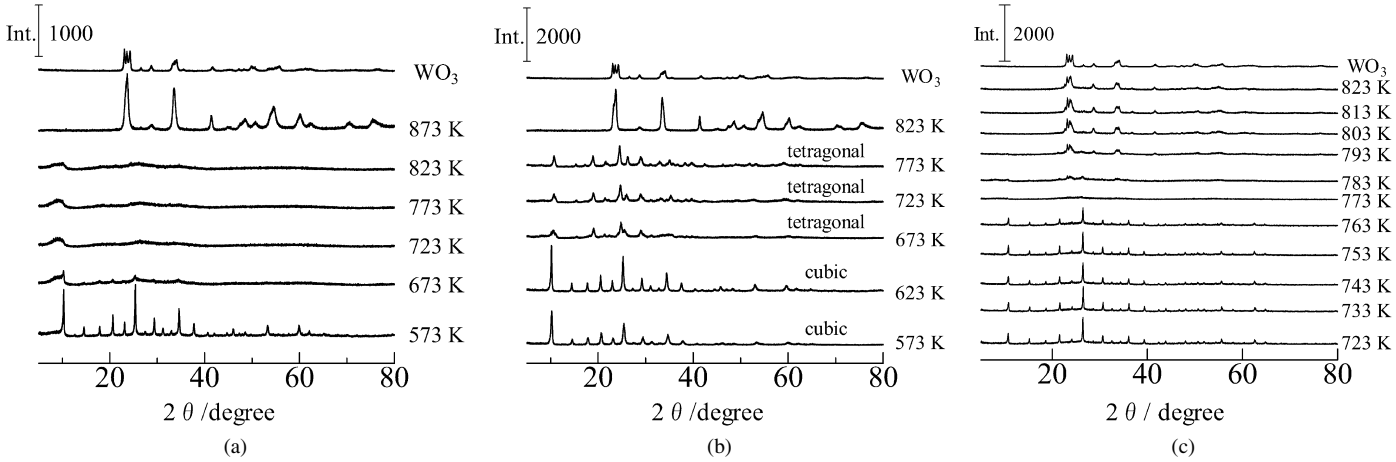

Fig. 2. XRD patterns of (a) HPNbW, (b) HPW, and (c) H_3PO_4–Nb_2O_5–WO_3 (Cat A) calcined at different temperatures.

3.2. Structural analysis of the decomposition process of HPAs

The structural aspects HPNbW in the course of the thermal transformation was followed by XRD, IR, and XAFS. The process was compared with those of HPW to reveal the effect of the Nb atom present in the Keggin structure. Figs. 2a and 2b show XRD patterns of HPNbW and HPW calcined at different temperatures, respectively. Fig. 2c shows the data for Cat A. The pattern of HPNbW was close to that of cubic HPW calcined at 573 K, indicating only slight modification of the crystal lattice of 12 W by replacement of an Nb atom. The XRD pattern of Cat A calcined at 723–763 K was close to that of cubic HPW, but the overall peak position shifted slightly to higher angles with respect to the HPNbW. The diffraction peaks of HPNbW disappeared on an increase in calcination temperature to 673–823 K, suggesting formation of the amorphous phase. The phenomenon agreed with the observation for Cat A calcined at 773–783 K in that the diffractions disappeared at these temperatures (Fig. 2c). On a further increase in calcination temperature to 873 K, intense diffractions assignable to the crystalline WO_3 appeared. The appearance of the diffractions meant that the rapid transformation of the amorphous oxide phase occurred in the temperature range of 823–873 K. On the other hand, diffraction patterns characteristic of the cubic phase were seen after calcination at 573 and 623 K over HPW. On an increase in calcination temperature to 673–773 K, the intensity of the diffraction peaks decreased due to the formation of a tetragonal phase, in accordance with previous findings [16]. Subsequent calcination at 773 K led to rapid transformation to the crystalline WO_3. The feature in XRD patterns of HPW was different from that of HPNbW in that the amorphous phase could not be seen until it was completely converted to the WO_3. Such a difference in the structural changes indicated that the presence of one Nb atom in the Keggin structure played an important role in generation of a partially decomposed HPA with an amorphous phase that emerged at 673–823 K.

Fig. 3 shows the FTIR spectra of HPNbW and HPW calcined at different temperatures. The peaks appeared at 1080, 985, 889, and 820 cm^{-1} could be assigned to the stretching vibrations of ν_{as}(P–O), ν_{as}(W=O), ν_{as}(W–O_c–W, corner-sharing),

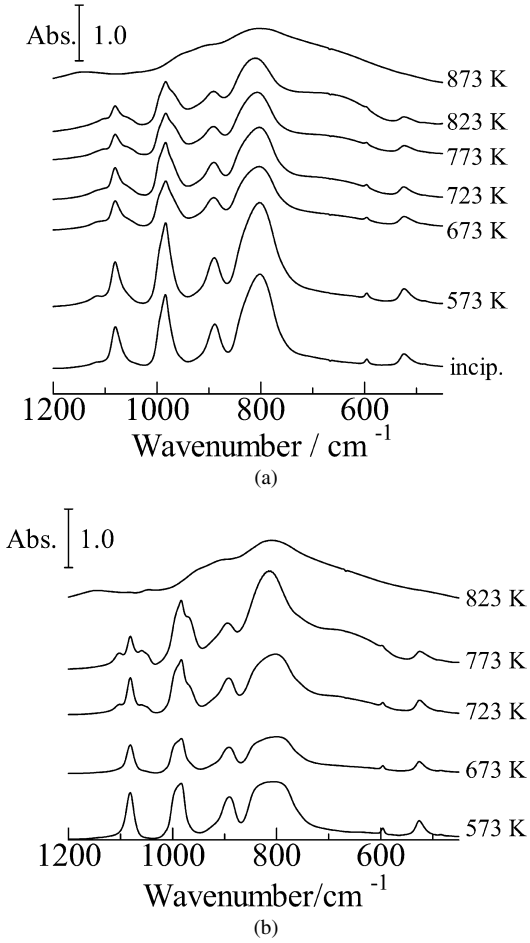

Fig. 3. FT-IR spectra of (a) HPNbW and (b) HPW calcined at different temperatures. The samples were diluted with KBr at a weight ratio of 1:10.

and ν_{as}(W–O_e–W, edge-sharing) in the spectra of HPAs calcined at 573 K, respectively [17]. For HPNbW, the intensity of the peaks decreased on calcination at 673 K, suggesting partial decomposition of Keggin framework at the temperature range studied. At the same time, two shoulders appeared at 1102 and 1059 cm^{-1} around the band corresponding to the ν_{as}(P–O) band. The splitting of the peak suggested the formation of la-

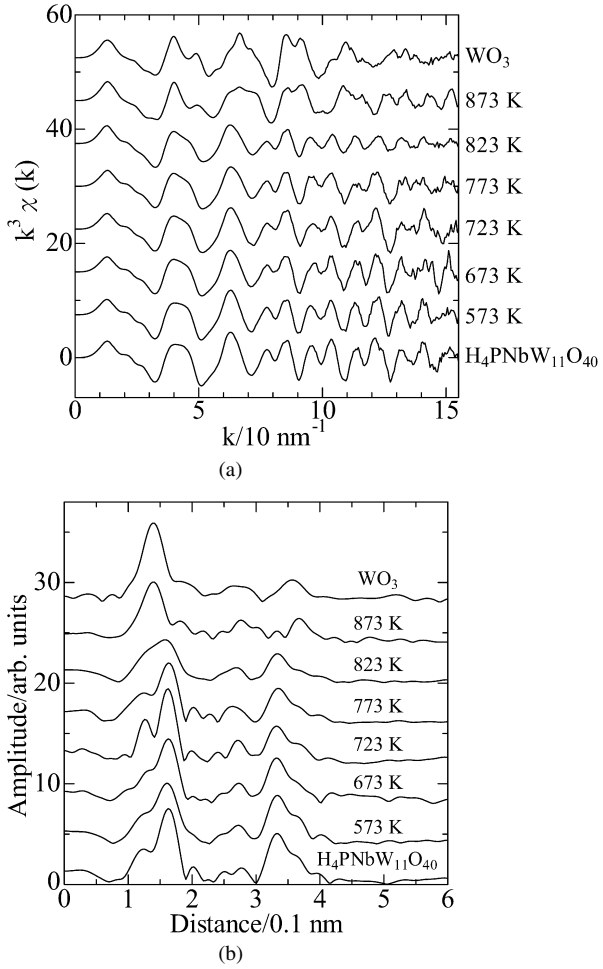

Fig. 4. W-L_3 edge EXAFS (a) $k^3\chi(k)$ and (b) their Fourier transforms of HPNbW calcined at different temperatures.

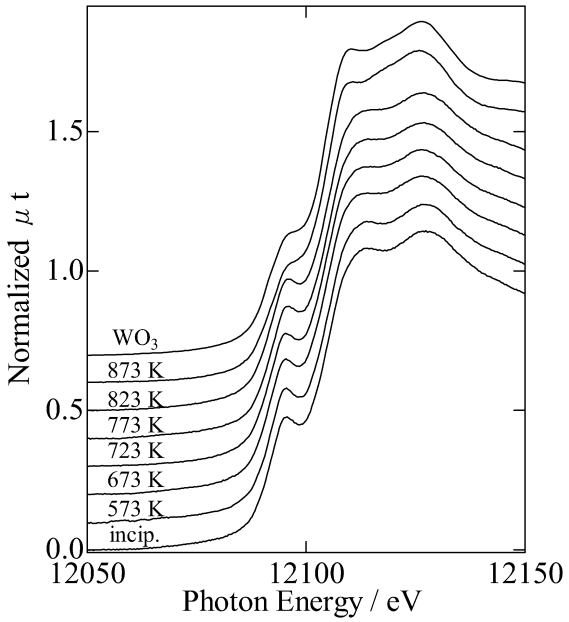

Fig. 5. W-L_1 edge XANES spectra of HPNbW calcined at different temperatures.

cunary (defect)-type structure, where a WO_3 unit was ruptured from the Keggin unit [18]. The spectrum became featureless on the sample calcined at 873 K due to the formation of crystalline WO_3. Likewise, splitting of the ν_{as}(P–O) band was observed over HPW calcined at 723–773 K, followed by the formation of WO_3 at 823 K. Such a splitting of the ν_{as}(P–O) band indicated that the disintegration of HPAs occurred via the rupture of fragmented units from HPAs.

W-L_3 edge EXAFS $k^3\chi(k)$ spectra and their Fourier transforms of HPNbW calcined at different temperatures are given in Figs. 4a and 4b, respectively. In the Fourier transforms of the intact HPNbW, two peaks appearing at 0.13 and 0.16 nm were assigned to the W=O and W–O bonds, respectively. In contrast, the peak at 0.3–0.4 nm comprised the overlapped W–O_c–W and W–O_e–W bonds. The intensity of the W–O–W bond decreased with increasing calcination temperature; then the bond disappeared at 873 K, and the spectrum became close to that of WO_3. Such facts were confirmed by changes in the rapid oscillations at 80–150 nm^{-1} in the $k^3\chi(k)$ spectra, which was characteristic of W–O–W bonds present in the Keggin structure. The decrease in the signal meant that the cleavage of W–O–W bonds progressed with increasing calcination temperature. Fig. 5 shows the W-L_1 edge XANES spectra corresponding to Fig. 4. The shape of the pre-edge peak appearing around 12.095 eV did not change up to 823 K. Then the intensity of the peak weakened until it became close to that of WO_3. The XAFS spectra indicated that the local symmetry around the W atoms was retained up to 823 K while the W–O–W bonds were partially ruptured, because the local symmetry around the W atoms reflected on the intensity of the pre-edge peak [19].

3.3. Acid properties of the thermally treated HPAs

Acid properties of the thermally treated HPAs were studied by means of NH_3 TPD coupled with IR spectra of adsorbed pyridine. Fig. 6 shows NH_3 TPD spectra of HPNbW and HPW calcined at different temperatures. A sharp NH_3 desorption peak was seen at 820–850 K over the intact HPAs. For HPNbW, on an increase in calcination temperature to 673 K, a broad peak emerged at 400–800 K along with the reduction in desorption of the sharp peak due to the HPNbW. The desorption from the HPNbW almost disappeared, and the broad peak remained over the samples calcined at 673 and 823 K. The desorption profile was close to that observed in Cat A calcined at 773–783 K as shown in Fig. 6c, which exhibited the highest activity in the Friedel–Crafts alkylations. Although a similar broad peak appeared over HPW calcined at 623–773 K, a sharp desorption peak due to the HPA remained until it was totally changed to WO_3 at 823 K. Comparing the TPD spectra of HPNbW and HPW shows that the presence of Nb atoms promoted formation of the novel acidity with a broad distribution. Fig. 7 shows the desorbed amount of NH_3 plotted as a function of calcination temperature. The amounts were determined based on the dry weight. For HPNbW, the broad desorption prevailed at the calcination temperature range of 673–823 K, where the desorption from HPNbW almost disappeared. The observation coincided with the XRD patterns in that the amorphous oxide prevailed at

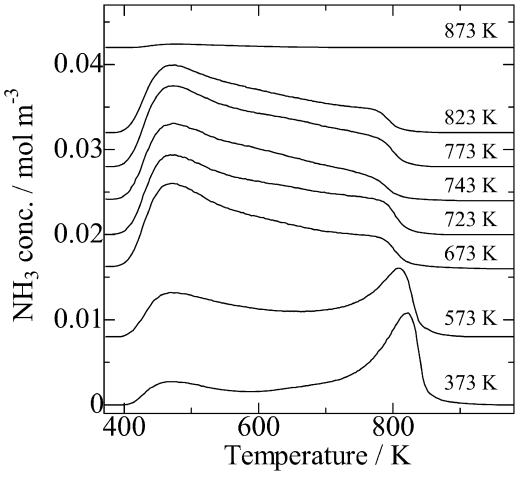

Fig. 6. Temperature programmed desorption of ammonia from (a) HPNbW, (b) HPW, and (c) H_3PO_4–WO_3–Nb_2O_5 (Cat A) calcined at different temperatures.

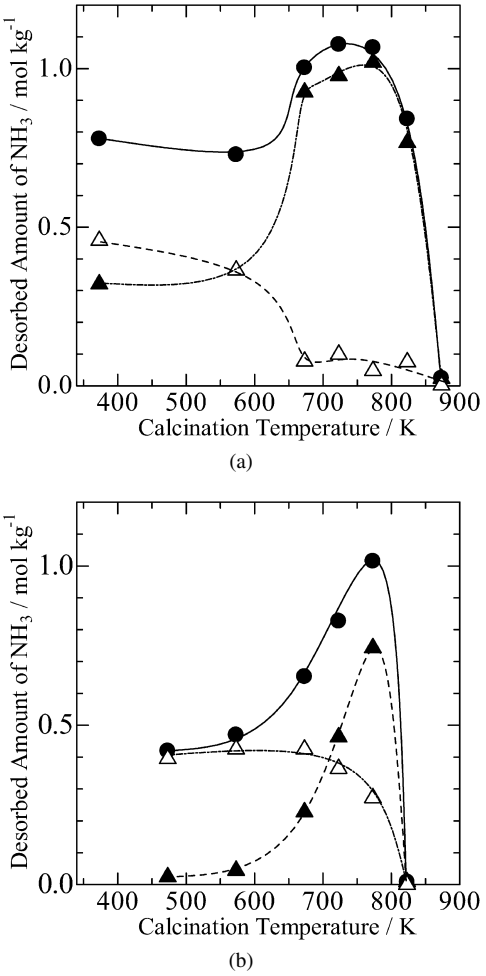

Fig. 7. Desorbed amount of ammonia from (a) HPNbW and (b) HPW calcined at different temperatures. (●) Total amount, (△) desorption from HPA, (▲) desorption from novel acid sites.

the corresponding temperature as described above. In contrast, broad desorption peaked at 773 K over HPW, but a considerable desorption from HPW remained even at this temperature. The fact suggests that the intermediate species derived from HPW consisted of the mixture of partially decomposed and intact HPW. It should be noted that the amount of NH_3 desorbed from undecomposed HPW calcined at 473 K was calculated to be 0.4 mol kg^{-1}. The value was as much as 42% of the expected acid amount present in the HPW. The rest of the adsorbed NH_3 likely reacted with WO_3 to afford tungsten nitride in the course of decomposition; thus, the desorbed amount of NH_3 was much smaller than the stoichiometry. In agreement with the assumption, simultaneous evolution of water was observed at the corresponding temperature. In another study, tungsten nitride was prepared at 833 K in a NH_3 stream using WO_3, and the temperature was close to that of the sharp desorption peak shown in Fig. 6b [20].

Figs. 8a and 8b show the IR spectra of pyridine adsorbed on the thermally treated HPNbW and HPW, respectively. The peak assignable to the Brønsted acid appeared at 1537 cm^{-1}, whereas that of Lewis sites was not observed round 1450 cm^{-1}. For HPNbW, the peak corresponding to the Brønsted acid sites was retained up to 773 K, but disappeared over the sample calcined at 873 K due to the formation of WO_3. The temperature was in agreement with that of the formation of WO_3 as shown in the XRD patterns (Fig. 2a) and IR spectra (Fig. 3a).

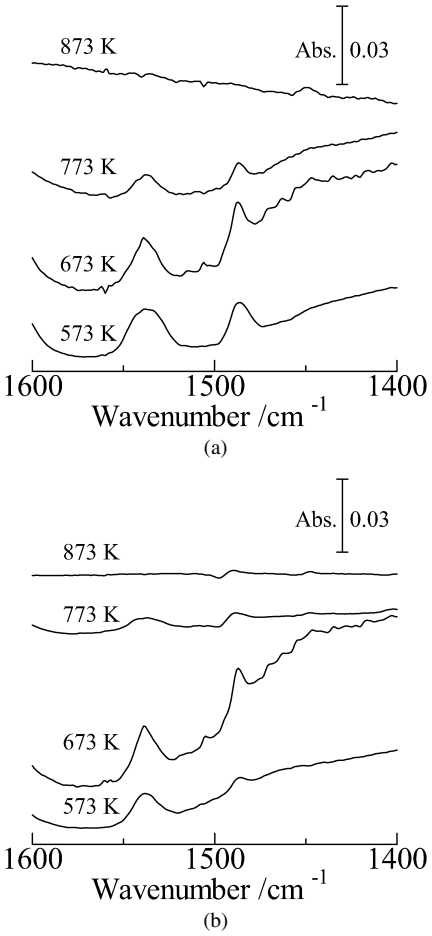

Fig. 8. IR spectra of pyridine adsorbed on (a) HPNbW and (b) HPW calcined at different temperatures.

3.4. Friedel–Crafts acylation of anisole with carboxylic acids over the catalyst derived from HPNbW (Cat B)

A catalyst was prepared from a mixed solution of HPNbW, ammonium tungstate, and niobic oxalate, followed by calcination in air at 773 K (Cat B). This catalyst can be the mimic of Cat A, taking into account that HPNbW was the primary precursor for the Cat A. Tables 1 and 2 give data for the acylation of anisole with benzoic acid and butyric acid over Cat B and Cat A, respectively. The reactions were also carried out over H-β zeolite for comparison, which has been used as a superior catalyst in the acylation of aromatic compounds using acid anhydrides [21]. The yields of C-acylated products (methoxybenzophenone and methoxybutyrophenone) were 55 and 81% in the reactions using benzoic acid and butanoic acid as acylating agents over Cat B, respectively, where the use in recycling was possible simply by filtration, as shown in the tables. The yields of aromatic ketones were higher than those over Cat A, thus confirming the improved catalytic performance with the use of HPNbW. Moreover, the yields were more than 2 times higher than those of H-β zeolite. For acylation with benzoic acid, concomitant formation of the O-acylated product (phenyl benzoate) was observed over H-β zeolite, whereas the C-acylated product was obtained almost selectively over Cat B. This indicates that Cat B was better than H-β in that the selective C-acylation proceeded with high efficiency.

Table 1
Data of the acylation of anisole and benzoic acid[a]

Catalyst	Benzoic acid conv. (%)	2-methoxybenzophenone yield (%)	4-methoxybenzophenone yield (%)	Phenyl benzoate yield (%)	Carbon material balance (%)
Cat B	77.2	2.7	52.1	6.0	84
Cat B[b]	69.4	3.0	51.3	4.2	89
Cat A	62.5	1.1	27.8	3.8	70
H-β[c]	74.4	0.0	19.7	18.6	64

[a] Cat A and Cat B designate H_3PO_4–WO_3–Nb_2O_5 and HPNbW–WO_3–Nb_2O_5, respectively; catalyst weight, 0.5 g; anisole, 10 g; benzoic acid, 2.0 mmol; temperature, 413 K; time, 3 h.
[b] Repeated reaction.
[c] Dehydrated at 573 K prior to use.

Table 2
Data of the acylation of anisole and butanoic acid[a]

Catalyst	Butanoic acid conv. (%)	4-methoxybutyrophenone yield (%)	Phenyl butylate yield (%)	Carbon material balance (%)
Cat B	96.7	80.5	1.7	84
Cat B[b]	97.9	81.9	1.4	84
Cat A	94.3	53.8	6.3	66
H-β[c]	67.8	41.8	0.9	74

[a] Cat A and Cat B designate H_3PO_4–WO_3–Nb_2O_5 and HPNbW–WO_3–Nb_2O_5, respectively; catalyst weight, 0.5 g; anisole, 10 g; butanoic acid, 2.0 mmol; temperature, 428 K; time, 3 h.
[b] Repeated reaction.
[c] Dehydrated at 573 K prior to use.

4. Discussion

4.1. Assignment of the extracts from Cat A based on the ^{31}P NMR

From the ^{31}P NMR study, the mixed heteropoly acid, $H_4PNbW_{11}O_{40}$ (HPNbW), was considered the primary precursor for the active species generated in Cat A. That is, in the ^{31}P NMR spectrum of the extracts from Cat A calcined at 673 K, the main peak appeared at −13.8 ppm, along with the peaks at −15.3 and −12.5 ppm. The peak of −15.3 ppm was straightforwardly assigned to HPW after comparison with an authentic sample. In the literature, the chemical shift (δ) of ^{31}P NMR spectrum of (n-Bu_4N)$_4$[$PNbW_{11}O_{40}$] (in an acetonitrile solution) was reported to be −12.7 ppm [22]. On the other hand, the chemical shift (δ) of (n-Bu_4N)$_3$[$PW_{12}O_{40}$] in an acetonitrile solution was reported to be −14.2 ppm [18]. Although the peak position shifted depending on the kind of cations (n-Bu_4N^+ or H^+) and solvents, these data suggested that the degree of chemical shift caused by the substitution of a W atom with one Nb atom was +1.5 ppm. In our case, the single peak appearing at −13.8 ppm in the ^{31}P NMR spectrum was +1.5 ppm higher than that of HPW (−15.3 ppm) [23]. The difference in the chemical shift was in good agreement with that between (n-Bu_4N)$_3$[$PW_{12}O_{40}$] and (n-Bu_4N)$_4$[$PNbW_{11}O_{40}$]. Actually, a single peak appeared at −13.8 ppm in the ^{31}P NMR spectrum

of HPNbW in a D_2O solution, as displayed in Fig. 1b. Taking into account these facts together with the result of ICP analysis, the peak at −13.8 ppm could be assigned to the HPNbW. In contrast, the position of the triple peaks (−12.3 ppm) was higher than that of single peak appearing at −13.8 ppm by +1.5 ppm. The difference agreed with the peak shift caused by substitution of a W atom in the Keggin structure with an Nb atom. Therefore, we assume that the triple peaks may be assignable to the $H_5PNb_2W_{10}O_{40}$ in which two W atoms in the Keggin unit of HPW were substituted with two Nb atoms. The existence of isomers with different configuration of Nb atoms likely caused the splitting of the peak. The Nb-containing heteropoly acid [$(t\text{-}Bu_4N)_4PNbW_{11}O_{40}$] has been synthesized by the insertion of an Nb atom into the gap of the lacunary (defect) structure [9,16]; however, the present study demonstrates that the heteropoly acid partially substituted with Nb atoms was readily formed simply by mixing the precursor solutions of P, Nb, and W in the acidic conditions. Such a facile incorporation of an Nb atom into the Keggin structure agreed with the fact that HPNbW was spontaneously generated in the preparation of Cat A, as shown here.

4.2. Formation of the active species in the H_3PO_4–WO_3–Nb_2O_5 (Cat A)

From the similarity in the structural and acidic properties coupled with NMR studies, the amorphous phase generated in the course of the thermal decomposition of HPNbW was supposed to be identical to the active species of Cat A that was realized at 773 K. As a matter of fact, no diffraction peaks appeared in the XRD patterns, and the NH_3 TPD spectra of Cat A calcined at 773 K were close to those of HPNbW calcined at 673–823 K (Fig. 6). Furthermore, the W-L_1 XANES and W-L_3 EXAFS of thermally-treated HPNbW agreed with that of Cat A, as reported earlier [13]. The fact was also supported by the excellent activity of the catalyst derived from HPNbW in the acylation of anisole with carboxylic acids, as shown in Tables 1 and 2. However, the reason for the shift in X-ray diffraction with respect to the dehydrated HPNbW is not yet straightforwardly understood. Although the formation of ammonium salt [$(NH_4)_4PNbW_{11}O_{40}$] was supposed, the possibility could be excluded taking into consideration that no desorption peaks of NH_3 appeared in the TPD of the intact Cat A without the exposure of NH_3. Another hypothesis was the inclusion of Nb or W cations in HPNbW, which led to expansion of the unit cell, thereby shifting the peak position to the higher angle.

It was found that the thermal decomposition process of HPNbW was significantly different from that of HPW. That is, an amorphous oxide was generated in the course of the thermal decomposition of HPNbW, whereas tetragonal H_3PWO_{40} remained over HPW until it was totally transformed into the crystalline WO_3, as evidenced by XRD. The tetragonal phase and the amorphous oxide likely coexisted in the HPW calcined at 673–773 K in practice, considering the simultaneous appearance of the broad and sharp desorption peaks in the TPD spectra (Fig. 6b) and splitting of the ν_{as}(P–O) band (Fig. 3b). The difference in the transformation process indicated that the presence of an Nb atom in the Keggin structure significantly affected the decomposition process. In previous studies, extensive effort was devoted to elucidating the structural transformation of Mo,V-mixed HPA (i.e., $H_4PVMo_{11}O_{40}$) [24]. Based on the Raman studies, Mestl et al. [25] reported that the transformation of $H_4PVMo_{11}O_{40}$ occurred via the expulsion of vanadyl and molybdenyl species from the Keggin structure to give fragments; then it disintegrated to give Mo_3O_{13} triads, followed by oligomerization to form MoO_3. The data for FTIR and XAFS spectra suggested the formation of a partially fragmented Keggin structure with maintenance of the local symmetry around the intact HPA. Taking these findings into account, the formation of Keggin fragments is likely to occur in a similar way as has been reported for the disintegration of $H_4PVMo_{11}O_{40}$.

Considering the surface area of Cat A (58 $m^2\,g^{-1}$), the WO_3–Nb_2O_5 mixed oxide generated simultaneously during preparation likely played a role as the support for fragments of HPNbW. As a matter of fact, the mixture of WO_3–Nb_2O_5 had a relatively high surface area (38–74 $m^2\,g^{-1}$) over the wide mixing ratio of WO_3 and Nb_2O_5 [26]. It can be supposed that the interaction between support oxides and fragmented HPNbW led to the formation of active species around the calcination temperature of 773 K.

5. Conclusion

In this study, we have attempted to assign the active component in the H_3PO_4–WO_3–Nb_2O_5 (Cat A) and follow its thermal decomposition process in terms of structure and acid properties. ^{31}P NMR of the extracts from Cat A revealed the spontaneous formation of heteropoly acids, in which HPNbW was found to be the primary component. The thermal transformation of HPNbW progressed via the formation of an amorphous oxide that had novel acidity with a broad distribution of acid strength. In marked contrast, the Keggin structure was partially retained over HPW until it was completely converted into crystalline WO_3. Such a difference in the thermal transformation process means that the presence of an Nb atom in Keggin structure played the crucial role in the formation of active species in Cat A. In agreement with these observations, the selective acylation of anisole with carboxylic acids proceeded over the HPNbW–WO_3–Nb_2O_5 catalyst (Cat B) to give C-acylated products with superior efficiency.

Acknowledgments

The present work was supported by a Grant-in-Aid for Scientific Research (KAKENHI) in Priority Area “Molecular Nano Dynamics” and Young Scientists (B) (18760584) from the Japanese Ministry of Education, Culture, Sports, Science and Technology. The authors thank Dr. Osamu Morikawa for ^{31}P NMR measurements.

References

[1] J.H. Clark, A.P. Kybett, D.J. Macquarrie, S.J. Barlow, P. Landon, Chem. Commun. (1989) 1353.

[2] B.M. Chaudary, M.L. Kantam, M. Sateesh, K.K. Rao, P.L. Santhi, Appl. Catal. A 149 (1997) 257.
[3] Y. Izumi, M. Ogawa, K. Urabe, Appl. Catal. A 132 (1995) 127.
[4] Á. Molnár, C. Keresszegi, B. Török, Appl. Catal. A 189 (1999) 217.
[5] M. Fournier, C. Feumi-Jantou, C. Rabia, G. Herve, S. Launay, J. Mater. Chem. 2 (1992) 971.
[6] D.P. Sawant, A.V. Nalini, E. Jacob, F. Lefebvrec, S.B. Halligudi, J. Catal. 235 (2005) 341.
[7] C. Marchal-Roch, R. Bayer, J.F. Moisan, A. Tézé, G. Hervé, Appl. Catal. A 114 (1996) 277.
[8] M. Akimoto, H. Ikeda, A. Okabe, E. Echigoya, J. Catal. 89 (1984) 196.
[9] C. Rocchiccioli-Deltcheff, M. Fournier, J. Chem. Soc. Faraday Trans. 87 (1991) 3913.
[10] D.P. Sawant, B.M. Devassy, S.B. Halligudi, J. Mol. Catal. A 217 (2004) 211.
[11] G.V. Shanbhag, B.M. Devassy, S.B. Halligudi, J. Mol. Catal. A 218 (2004) 67.
[12] J.-M. Tatibouët, C. Montalescot, K. Brückman, J. Haber, M. Che, J. Catal. 169 (1997) 22.
[13] K. Okumura, K. Yamashita, M. Hirano, M. Niwa, J. Catal. 234 (2005) 300.
[14] K. Okumura, K. Yamashita, M. Hirano, M. Niwa, Chem. Lett. 34 (2005) 716.
[15] H.S. Booth (Ed.), Inorg. Synth., vol. 1, McGraw-Hill, New York, 1939.
[16] M. Fournier, C. Feumi-Hantou, C. Rabia, G. Hervé, S. Launay, J. Mater. Chem. 2 (1992) 971.
[17] T. Okuhara, N. Mizuno, M. Misono, Adv. Catal. 41 (1996) 113.
[18] J.A. Gamelas, F.A.S. Couto, M.C.N. Trovão, A.M.V. Cavaleiro, J.A.S. Cavaleiro, J.D.P. de Jesus, Thermochim. Acta 326 (1999) 165.
[19] A. Kuzmin, J. Purans, J. Phys. Condens. Matter 5 (1993) 9423.
[20] R.C.V. McGee, S.K. Bej, L.T. Thompson, Appl. Catal. A 284 (2005) 139.
[21] K. Smith, Z. Zhenhua, P.K.G. Hodgson, J. Mol. Catal. A 134 (1998) 121.
[22] E. Tadkov, E.H. Beer, Polydedron 14 (1995) 2139.
[23] A. Proust, M. Fournier, R. Thouvenot, P. Gouzerh, Inorg. Chim. Acta 215 (1994) 61.
[24] C. Marchal-Roch, R. Bayer, J.F. Moisan, A. Tézé, G. Hervé, Appl. Catal. A 114 (1996) 277.
[25] G. Mestl, T. Ilkenhans, D. Spielbauer, M. Dieterle, O. Timpe, J. Kröhnert, F. Jentoft, H. Knözinger, R. Schlögl, Appl. Catal. A 210 (2001) 13.
[26] K. Yamashita, M. Hirano, K. Okumura, M. Niwa, Catal. Today 118 (2006) 385.